

This discussion paper is/has been under review for the journal *Atmospheric Chemistry and Physics (ACP)*. Please refer to the corresponding final paper in *ACP* if available.

**Vertical distribution
of sub-micron
aerosol chemical
composition**

W. T. Morgan et al.

Vertical distribution of sub-micron aerosol chemical composition from North-Western Europe and the North-East Atlantic

W. T. Morgan¹, J. D. Allan^{1,2}, K. N. Bower¹, G. Capes¹, J. Crosier^{1,2},
P. I. Williams^{1,2}, and H. Coe¹

¹Centre for Atmospheric Science, University of Manchester, Manchester, UK

²National Centre for Atmospheric Science, University of Manchester, Manchester, UK

Received: 6 March 2009 – Accepted: 30 March 2009 – Published: 6 April 2009

Correspondence to: W. T. Morgan (william.morgan@postgrad.manchester.ac.uk)

Published by Copernicus Publications on behalf of the European Geosciences Union.

Title Page

Abstract

Introduction

Conclusions

References

Tables

Figures

⏪

⏩

◀

▶

Back

Close

Full Screen / Esc

Printer-friendly Version

Interactive Discussion

Abstract

A synthesis of UK based airborne in-situ measurements of aerosol properties representing air masses from North-West Europe and the North-East Atlantic is presented. The major focus of the study is the vertical distribution of sub-micron aerosol chemical composition. Vertical profiles are derived from a Quadrupole Aerosol Mass Spectrometer (Q-AMS). Background sub-micron aerosol vertical profiles are identified and are primarily composed of organic matter and sulphate aerosol. Such background conditions occurred predominantly during periods associated with long-range air mass transport across the Atlantic. These instances may serve as useful model input of aerosol to Western Europe. Increased mass concentration episodes are coincident with European outflow and periods of stagnant/recirculating air masses. Such periods are characterised by significantly enhanced concentrations of nitrate aerosol relative to those of organic matter and sulphate. Periods of enhanced ground level PM_{2.5} loadings are coincident with instances of high nitrate mass fractions measured on-board the aircraft, indicating that nitrate is a significant contributor to regional pollution episodes. The vertical structure of the sulphate and organic aerosol profiles were shown to be primarily driven by large-scale dynamical processes. The vertical distribution of nitrate is likely determined by both dynamic and thermodynamic processes, with chemical partitioning of gas phase precursors to the particle phase occurring at lower temperatures at the top of the boundary layer. Such effects have profound implications for the aerosol's lifetime and subsequent impacts, highlighting the requirement for accurate representation of the aerosol vertical distribution.

1 Introduction

Uncertainty surrounding the impact of atmospheric aerosol is a major barrier to accurate prediction of future anthropogenically induced climate change (Forster et al., 2007). Human activity has increased the atmospheric aerosol concentration, which is

ACPD

9, 9117–9150, 2009

Vertical distribution of sub-micron aerosol chemical composition

W. T. Morgan et al.

Title Page

Abstract

Introduction

Conclusions

References

Tables

Figures

⏪

⏩

◀

▶

Back

Close

Full Screen / Esc

Printer-friendly Version

Interactive Discussion

**Vertical distribution
of sub-micron
aerosol chemical
composition**W. T. Morgan et al.

[Title Page](#)[Abstract](#)[Introduction](#)[Conclusions](#)[References](#)[Tables](#)[Figures](#)[⏪](#)[⏩](#)[◀](#)[▶](#)[Back](#)[Close](#)[Full Screen / Esc](#)[Printer-friendly Version](#)[Interactive Discussion](#)

known to significantly alter the Earth's radiative equilibrium on regional to global scales (e.g. Haywood and Boucher, 2000). The direct and indirect aerosol radiative forcing strongly depends upon aerosol properties as a function of height (e.g. Forster et al., 2007). The chemical composition of the aerosol is one such property. Global aerosol models require direct representation of aerosol chemical composition (e.g. Textor et al., 2006). The AeroCom exercise (Kinne et al., 2006; Schulz et al., 2006; Textor et al., 2006) established significant differences between participating models in terms of vertical aerosol dispersion (Textor et al., 2006). This variance contributes significantly to uncertainties in estimates of aerosol lifetimes in the atmosphere, which in turn impacts their climate effect. Ground based measurements of aerosol composition are numerous, facilitating model comparisons at the surface. However, in-situ vertical profiles of aerosol chemical speciation are sparse. Consequently, there is a need for high-quality measurement data of aerosol properties as a function of altitude.

Traditional methods for aerosol composition measurements, such as filter based techniques, are incapable of providing highly time resolved vertical profiles. Novel on-line techniques are required to accurately measure the vertical distribution of aerosol composition. Examples of such instruments are the Particle-Into-Liquid Sampler (PILS, Weber et al., 2001) and the Aerodyne Aerosol Mass Spectrometer (AMS, Jayne et al., 2000; Canagaratna et al., 2007). Both have demonstrated the capability to quantitatively measure aerosol composition from airborne platforms (Bahreini et al., 2003; Lee et al., 2003; Orsini et al., 2003; Crosier et al., 2007).

Dynamical processes control the advection of aerosol and their precursors to the sampling region. This has been shown to modify the concentration and relative distribution of chemical species of sub-micron aerosol in the planetary boundary layer (e.g. Bahreini et al., 2003; Schneider et al., 2006; Crosier et al., 2007). A complicating factor regarding the aerosol vertical distribution is the role of chemical, rather than large-scale dynamical effects. Ammonium nitrate formation close to the top of the boundary layer is an example of this (Neuman et al., 2003; Morino et al., 2006). This phenomenon is driven by partitioning between the gas and particle regimes, which

is strongly dependent upon temperature and relative humidity (Stelson and Seinfeld, 1982; Mozurkewich, 1993). The partitioning is biased towards the particle phase at lower temperatures and high relative humidity.

Characterisation of aerosol processes and properties on regional scales is paramount in order to assess regional air quality and to predict future changes in atmospheric variables, such as temperature and precipitation. Atmospheric processes over the UK provide a useful test case, as aerosol properties are expected to be significantly modulated by the dominant meteorological synoptic situation. As a result, the UK is representative of a much wider region encompassing North-Western Europe and the North-East Atlantic. Abdalmogith and Harrison (2005) found significant variations in sulphate and nitrate at two ground based locations in the UK due to differing air mass histories. Higher concentrations were associated with south-easterly and easterly back trajectories originating from continental Europe. Coe et al. (2006) showed that, during marine conditions, background input of sulphate and organic aerosol into Western Europe were between 0.5 and 1.0 $\mu\text{g sm}^{-3}$. Thus variability in mass concentrations and the relative fraction of chemical species is well established.

This paper presents measurements of aerosol properties in the UK region from the UK Facility for Airborne Atmospheric Measurements (FAAM) BAe-146 research aircraft. The vertical distribution of aerosol chemical composition is the major focus of the study. The influence of air mass history upon the aerosol mass concentration and relative chemical components will be investigated based upon a back trajectory cluster analysis. High pollution episodes identified via the UK ground-based measurement network will be examined using the aircraft data coupled with the back trajectory analysis.

**Vertical distribution
of sub-micron
aerosol chemical
composition**W. T. Morgan et al.

[Title Page](#)[Abstract](#)[Introduction](#)[Conclusions](#)[References](#)[Tables](#)[Figures](#)[⏪](#)[⏩](#)[◀](#)[▶](#)[Back](#)[Close](#)[Full Screen / Esc](#)[Printer-friendly Version](#)[Interactive Discussion](#)

2 Methodology

2.1 Sampling platform and instrumentation

The FAAM BAe-146 research aircraft has a typical range of over 3000 km and a height ceiling of over 10.5 km. The aircraft's science speed is approximately 100 m s^{-1} . Profile ascents and descents are made at approximately 150 m per minute below 1 km and at 300 m per minute above 1 km. The aircraft houses a suite of instruments capable of resolving aerosol properties. Only instruments used in this analysis are discussed further. Number size distributions are measured via a wing-mounted Particle Measurement Systems (PMS) Passive Cavity Aerosol Spectrometer Probe 100X (PCASP, Liu et al., 1992; Strapp et al., 1992). The instrument optically counts particles between 0.1– $3 \mu\text{m}$ diameter across 15 channels. Particle number concentrations greater than 3 nm were measured by a TSI Inc. Ultrafine Condensation Particle Counter (CPC, Model 3025A). Furthermore, the facility provides aircraft position information and measurements of standard atmospheric variables, such as temperature and relative humidity.

Measurements made by the Aerodyne Quadrupole Aerosol Mass Spectrometer (Q-AMS) will be the major focus of this study. The Q-AMS has demonstrated the capability to quantitatively measure the size-resolved chemical composition of non-refractory particulate matter of widely varying volatility (Jayne et al., 2000; Allan et al., 2003; Jimenez et al., 2003). Furthermore, it is capable of providing such quantitative measurements with high time resolution in a range of environments from different platforms, such as aircraft. Standard operating practises are followed for ambient sampling (Jimenez et al., 2003), data quantification (Allan et al., 2003) and mass spectrum deconvolution (Allan et al., 2004). Recent laboratory evidence (Matthew et al., 2008) indicates that the AMS collection efficiency is significantly modulated by particle phase. Here a collection efficiency correction is applied following the principle developed by Crosier et al. (2007), which takes into account the nitrate content of the sampled aerosol.

Crosier et al. (2007) detailed the operating practises and sampling strategy for the Q-AMS on-board the BAe-146, which is summarised here. The Q-AMS was connected

Vertical distribution of sub-micron aerosol chemical composition

W. T. Morgan et al.

Title Page

Abstract

Introduction

Conclusions

References

Tables

Figures

◀

▶

◀

▶

Back

Close

Full Screen / Esc

Printer-friendly Version

Interactive Discussion

**Vertical distribution
of sub-micron
aerosol chemical
composition**W. T. Morgan et al.

[Title Page](#)[Abstract](#)[Introduction](#)[Conclusions](#)[References](#)[Tables](#)[Figures](#)[⏪](#)[⏩](#)[◀](#)[▶](#)[Back](#)[Close](#)[Full Screen / Esc](#)[Printer-friendly Version](#)[Interactive Discussion](#)

to a Rosemount inlet (Foltescu et al., 1995) via approximately 0.7 m of stainless steel tubing. Samples were introduced at ambient pressure and sub-micron particle losses are considered negligible for the operating altitudes considered by this study (Zhang et al., 2002). The aerosol sample introduced to the Q-AMS is considered dry. This is due to the coupled effect of the aircraft cabin temperature exceeding ambient temperatures and additional ram heating due to the decelerating sample airflow. As the flow is controlled by a critical orifice, increases in altitude cause decreases in the standard flow rate into the instrument. This results in an increase in the species specific detection limits of the Q-AMS. Mass concentration values are reported as micrograms per standard cubic metre i.e. at a temperature of 273.15 K and pressure of 1013.25 hPa. Q-AMS data points are reported as 30 s time intervals.

The Q-AMS comprises three fundamental sections: the particle beam generation region; the aerodynamic sizing region and the particle composition region. The particle beam generation comprises a 130 μm critical orifice, which controls the flow rate into the instrument. An aerodynamic lens system (Liu et al., 1995a,b) is used to collimate the sampled air into a narrow particle beam with 100% transmission for 40–700 nm vacuum aerodynamic diameter (DeCarlo et al., 2004) particles. However, at reduced pressure, the transmission efficiency through the lens may be shifted towards smaller particle sizes. Upon exiting the lens system, the gas undergoes a supersonic expansion and the particle's velocity increases as a function of its vacuum aerodynamic diameter. The particle's size may thus be inferred via measurement of its flight time through the length of the vacuum chamber. Particles then impact upon a resistively heated surface at a temperature of approximately 550°C where they undergo flash vaporisation. The resultant gas is then ionized via 70 eV electrons emitted by a Tungsten filament. A quadrupole mass spectrometer then classifies the sample ions according to a specific mass-to-charge (m/z) ratio. An electron multiplier detects the resultant ion signal. The aerosol beam is blocked periodically to obtain a mass spectrum of the background in the vacuum chamber. This is subtracted from the mass spectrum of the aerosol laden air to remove the background component. A zero particle filter can be

used to determine the detection limit of the instrument intermittently from the standard error of the signal fluctuating about zero.

2.2 Location of measurements

The present analysis uses data from 41 flights based in the UK region. The period covered is from 5 April 2005 to 27 September 2006. The full dataset for both the Q-AMS data and flight parameters is available from the British Atmospheric Data Centre (BADC, <http://badc.nerc.ac.uk>). The flights are drawn from several projects associated with aerosol and cloud studies. A total of 339 profiles were identified from these flights. Low-level (defined as those below 2.5 km) Straight Level Runs (SLRs) were also identified. Size distributions from the PCASP were available on 82 SLRs. The location of these profiles and SLRs are summarised in Fig. 1. Predominantly, the measurements presented are located over marine areas due to air traffic restrictions placed upon the aircraft. Profiles and SLRs were grouped into “sectors” encompassing a 2° by 2° latitude/longitude grid based on their median longitude and latitude point. The sectors were assigned on a grid from 48–60° N and between 8° W and 4° E.

2.3 Back trajectory cluster analysis

Three dimensional air mass back trajectories were derived from European Centre for Medium-Range Weather Forecasts (ECMWF) wind fields. The start points of the trajectories of each profile were defined from the latitude and longitude coordinates of the centre of the sector associated with that profile. The initialisation start time was chosen as 12:00 UTC as this time corresponded most closely to the airborne operations in all cases. Trajectories were established for the previous three days at 6 hourly intervals. Three vertical levels were chosen; 950 hPa, 750 hPa and 500 hPa. A total of 159 back trajectories were generated. The latitude and longitude coordinates were converted to km north and km east, respectively (assuming a spherical Earth), whilst the pressure was retained as hPa.

Vertical distribution of sub-micron aerosol chemical composition

W. T. Morgan et al.

Title Page

Abstract

Introduction

Conclusions

References

Tables

Figures

⏪

⏩

◀

▶

Back

Close

Full Screen / Esc

Printer-friendly Version

Interactive Discussion

Back trajectories were processed using a custom made cluster analysis routine, based on the method described in Cape et al. (2000). An average linkage method was used to compute the squared distance between each trajectory at individual time steps using Eq. (1):

$$d(x_i, x_j) = \sum_k \left\{ (x_{ki} - x_{kj})^2 + (y_{ki} - y_{kj})^2 + (p_{ki} - p_{kj})^2 \right\} \quad (1)$$

where x_{ki} , y_{ki} , p_{ki} are coordinates of trajectory x_i at each time point k . The average distance between two trajectories, x_i and x_j , are calculated. At the start of the analysis, each trajectory is assigned to its own cluster. All possible pairs are evaluated with the two clusters with the smallest average distance between their members joining. An iterative process is employed until all trajectories reside in one cluster. The “optimum” number of clusters may then be selected. The procedure seeks to minimize within cluster variance and maximize between cluster variance (Cape et al., 2000). This method has been shown to be the most appropriate means of classifying meteorological data (Kalkstein et al., 1987).

The number of clusters to retain for analysis is subjective (Kalkstein et al., 1987). Several indicators may be used in order to select an appropriate number of clusters, N . One such indicator is the coefficient of determination, R^2 , which is defined as the proportion of the variance explained by the current number of clusters at each iteration step:

$$R^2 = 1 - \frac{\sum (\text{within cluster variance})}{N (\text{variance of all trajectories})} \quad (2)$$

where the first sharp decrease can be used as a subjective indicator of the number of clusters to retain (Kalkstein et al., 1987). The Root Mean Square (RMS) distance between clusters may also be used, where an increase signifies that two dissimilar clusters have been joined (Cape et al., 2000). Similarly to Cape et al. (2000), an indication of the number of major clusters is defined based on the number of clusters

**Vertical distribution
of sub-micron
aerosol chemical
composition**W. T. Morgan et al.

[Title Page](#)[Abstract](#)[Introduction](#)[Conclusions](#)[References](#)[Tables](#)[Figures](#)[⏪](#)[⏩](#)[◀](#)[▶](#)[Back](#)[Close](#)[Full Screen / Esc](#)[Printer-friendly Version](#)[Interactive Discussion](#)

containing more than 3% of the total number of trajectories. Figure 2 displays the change in these measures as a function of the number of clusters for the trajectories initialized at 750 hPa. A comparison between R^2 and RMS indicates that the initial number of clusters to retain is 12 based on a “step” in both statistics. The number of clusters was reduced to 5 after examination of the trajectories and average 850 hPa geopotential height fields for each of the 12 clusters. The clustering routine was also run for the 950 hPa and 500 hPa pressure levels to ensure vertical consistency, which resulted in a similar solution. Furthermore, the 750 hPa solution was found to be similar when the analysis was performed on five day back trajectories. Consequently, the subsequent discussion and analysis will be based upon the three day back trajectories initialized at 750 hPa.

The five cluster solution derived from the back trajectory analysis is summarised in Table 1 and Fig. 3. To facilitate interpretation of the cluster solutions, average geopotential height fields were generated from ECMWF operational analysis data. These are included along with the full back trajectory solutions for each cluster in the supplementary material section: <http://www.atmos-chem-phys-discuss.net/9/9117/2009/acpd-9-9117-2009-supplement.pdf>. Cluster 1 encompasses three initial clusters, which were dominated by westerly, south-westerly and north-westerly trajectories. Thus this cluster was prescribed as the Atlantic cluster. The associated synoptic conditions are representative of westerly flow into the UK region and Northern Europe, consistent with the clusters mean back trajectory. Cluster 2 comprised two clusters made of easterly back trajectories from Northern to Central Europe. The geopotential height field shows a relatively weak anticyclonic pressure system over the UK with outflow from Northern Europe. Cluster 3 comprised air masses originating from Spain and France. The synoptic situation is characterised by high pressure over Southern/Central Europe and over the Central Atlantic. A low pressure system is situated off the west coast of Ireland in the North Atlantic. This results in broadly southerly flow consistent with the back trajectories. Cluster 4 comprised largely north-westerly back trajectories with a cyclonic rotational component distinct from the previous north-westerly trajec-

**Vertical distribution
of sub-micron
aerosol chemical
composition**

W. T. Morgan et al.

Title Page

Abstract

Introduction

Conclusions

References

Tables

Figures

⏪

⏩

◀

▶

Back

Close

Full Screen / Esc

Printer-friendly Version

Interactive Discussion

5 tories, which were assigned to cluster 1. The geopotential height field is consistent with the interpretation from the back trajectories. Cluster 5 comprises back trajectories centred on the UK representing a relatively stagnant air mass. This is in agreement with the geopotential height field that displays a ridge of high pressure situated over the UK. Cluster 3 is distinct from the other clusters in terms of its vertical displacement as it is the only cluster which ascends during its transit to the UK region.

3 UK aerosol chemical composition profiles

3.1 Full dataset characterisation

10 Summary statistics and individual data points of aerosol chemical composition measured by the Q-AMS for the full profile dataset are presented in Figs. 4 and 5. The black raw data points are those which fall above the 2σ profile for each individual species, where 2σ is defined as two times the standard error for a 30 s average data point. These are calculated for 500 m altitude bins when the detected signal by the Q-AMS is close to zero. In particular, resolving low mass concentrations for organics and ammonium is difficult due to the signal-to-noise constraints of the Q-AMS. The variability and indication of the number of points within an altitude bin is represented by calculating the variability about the mean value in each bin. This is defined as the Mean Absolute Error (MAE) divided by the square root of the number of points, n , in an altitude bin. MAE is defined as:

$$20 \text{ MAE} = \frac{1}{n} \sum_{i=1}^n |e_i| \quad (3)$$

where e_i is the absolute difference between the mean bin value and the raw data value. The profiles are categorised by a relatively small Inter Quartile Range (IQR, defined as the difference between the 75th and 25th percentile) with sulphate and organics having an IQR between $0\text{--}2 \mu\text{g sm}^{-3}$ below 3000 m. This is interpreted as background mass

Vertical distribution of sub-micron aerosol chemical composition

W. T. Morgan et al.

Title Page

Abstract

Introduction

Conclusions

References

Tables

Figures

⏪

⏩

◀

▶

Back

Close

Full Screen / Esc

Printer-friendly Version

Interactive Discussion



concentration levels. The higher concentrations above the 75th percentile are likely associated with pollution plumes. Nitrate mass concentrations are generally much lower than organics and sulphate with the peak concentration for the 75th percentile being less than $1.0 \mu\text{g sm}^{-3}$. However, when nitrate is enhanced, it is a major constituent of the sub-micron mass detected by the AMS. Ammonium is broadly similar to the sulphate and nitrate profiles due to its association with those species in the form of ammonium sulphate and ammonium nitrate, respectively.

Above 4000 m, data coverage is much more limited and the mass of aerosol is significantly decreased. Sulphate and nitrate mass concentrations are low with little variability. In contrast, organic mass is characterised by low or negative mass concentrations, punctuated by significantly enhanced concentrations above the 2σ profile. The 25th percentile for both the organics and ammonium are negative above 4000 m. The organic mass median profile is relatively low (less than $1.0 \mu\text{g sm}^{-3}$), whilst the 75th percentile profile above approximately 7000 m is higher than the corresponding profile in the boundary layer. The error about the mean in each bin is significantly enhanced compared with those below 4000 m. This suggests large variability coupled with potentially low statistical significance above this level. Above approximately 5000 m, the variability and lower number of data points results in the error about the mean being more than two times greater than values in the boundary layer. The variability in the values for nitrate and sulphate are much lower due to improved SNR for these species at higher altitudes compared with organic mass. In order to establish how representative such data is, the counting error is determined based on the binned total number concentration profile from the CPC. For data below 9500 m, the counting error is substantially less (typically less than 5%) than the standard deviation in each bin. Above 9500 m, the counting error is between 10–20% of the standard deviation in each bin. This indicates that the total number of particles sampled is significant and that the measured mass loading is representative. However, in the case of the organic mass outside of the boundary layer, the uncertainty increases substantially.

**Vertical distribution
of sub-micron
aerosol chemical
composition**W. T. Morgan et al.

[Title Page](#)[Abstract](#)[Introduction](#)[Conclusions](#)[References](#)[Tables](#)[Figures](#)[⏪](#)[⏩](#)[◀](#)[▶](#)[Back](#)[Close](#)[Full Screen / Esc](#)[Printer-friendly Version](#)[Interactive Discussion](#)

3.2 Aerosol properties as a function of air mass history

The clusters identified in Sect. 2.3 present an opportunity to compare aerosol properties in differing air masses. The Atlantic cluster represents a largely clean air mass entering the UK region. The cluster is representative of the input of aerosol to Western Europe during such conditions. When sampling in coastal areas downwind of the UK, such an air mass will also be associated with pollution originating from the UK itself. The easterly cluster is characteristic of pollution transport from Northern/Central Europe. Some additional input from the UK region may also occur depending upon the location of the sampling. The stagnant air mass cluster will be examined also. The southerly and northerly clusters are under-sampled relative to the other clusters. Thus these are omitted from the subsequent analysis which will focus on the three dominant transport patterns.

Figure 6 indicates that aerosol concentrations are enhanced for the easterly cluster compared with the Atlantic cluster. This is particularly evident in the case of nitrate, which is very low for the Atlantic cluster, whereas for the easterly condition it is a substantial component of the sub-micron mass. This is consistent with European pollution outflow leading to an enhancement in the mass concentration of nitrate. Sulphate and organic concentrations are also enhanced due to the large availability of sources in continental Europe. Concentrations for the stagnant condition are increased relative to the Atlantic case. This is consistent with the general build-up of pollution during a stagnant air mass episode.

Generally, the organics and sulphate profiles do not exhibit strong gradients within the boundary layer itself. Nitrate displays strong coupling with NO_x close to the surface (not shown), decreasing to close to zero between 1000–1500 m. Such features are primarily a result of the advection of pollution plumes driven by the larger scale dynamical situation. Above 1500 m, a secondary maximum occurs. Potentially, this is a result of partitioning between the gas and particulate phase at lower temperatures and enhanced relative humidity. This is suggestive of nitrate formation being primarily

Vertical distribution of sub-micron aerosol chemical composition

W. T. Morgan et al.

Title Page

Abstract

Introduction

Conclusions

References

Tables

Figures

⏪

⏩

◀

▶

Back

Close

Full Screen / Esc

Printer-friendly Version

Interactive Discussion

driven by the thermodynamics in this atmospheric layer.

Number-size distributions and estimated volume size distributions from the PCASP are shown in Fig. 7. These are extracted from the SLRs identified in Fig. 1 and the relevant number of SLRs for each cluster is shown in Table 1. The first two channels from the PCASP are omitted as these have been known to experience elevated levels of intermittent electronic noise. Consequently, the distributions shown are from 0.15 μm to 3 μm . The shape of the distributions is broadly similar. The number-size distributions all peak between 0.15 μm and 0.3 μm . The volume distributions for the Atlantic, easterly and stagnant air masses peak at approximately 0.3 μm . However, the distributions display significant differences between their concentrations, particularly above 0.3 μm . Due to the relatively small number of SLRs for the stagnant cluster, direct comparisons will be drawn between the easterly and Atlantic only. Based on the volume-convolved distributions, the majority of the mass sampled by the Q-AMS will be for particles smaller than 600 nm. The volume distributions indicate the presence of significant super-micron aerosol. This is likely composed of primary particles and is not discussed further in this paper.

The easterly number-size and volume distributions are enhanced compared to the Atlantic distribution. This is particularly pronounced above 0.3 μm . This is consistent with the higher mass concentrations observed in the profile data for the easterly condition. Newly formed secondary species condense upon available surfaces, further increasing the volume of material at larger sizes. Consequently, the distinctions between the distributions for the easterly and Atlantic clusters are consistent with the Q-AMS profile data. The size distributions from this analysis are consistent with those obtained by Osborne and Haywood (2005) during the ACE-2 experiment within the instrument's uncertainty. Osborne and Haywood (2005) also noted an enhancement in the accumulation mode as a result of aerosol aging.

**Vertical distribution
of sub-micron
aerosol chemical
composition**

W. T. Morgan et al.

Title Page

Abstract

Introduction

Conclusions

References

Tables

Figures

⏪

⏩

◀

▶

Back

Close

Full Screen / Esc

Printer-friendly Version

Interactive Discussion

3.3 Pollution episodes and comparison with the surface-based network

In order to study the characteristics of high pollution episodes, several flights have been selected based on elevated measurements of $\text{PM}_{2.5}$ mass concentrations from the UK surface-based measurement network. The aircraft data is compared with a rural monitoring station in Harwell, Oxfordshire ($51^{\circ}36'0''$ N, $1^{\circ}17'24''$ W) in the South East of the UK. The site is marked in Fig. 1. This station was selected due to its location away from major population centres, roads or industrial sources. Measurements made at the site are therefore largely representative of regional aerosol concentrations. Thus it provides an indication of the general pollution situation, which is independent of the measurements made on the aircraft. The data is provided by the UK Air Quality Archive website (<http://www.airquality.co.uk/archive/index.php>) for the period covered by the analysis, which runs from 5 April 2005 to 27 September 2006. Daily mean values at Harwell were available for 40 out of 41 flights and were ranked according to total mean loading. The data is summarised by a frequency distribution shown in Fig. 8. The distribution for the entire flying period and the distribution for the flying days are investigated using a two-sample T-test on unpaired means in order to discern whether the distributions are statistically different. The null hypothesis is that the population means are equal at the 0.05 (5%) significance level. The T-statistic for the distributions is 1.930, with a p-value of 0.101. Consequently, the null hypothesis may not be rejected at the 5% level and the flights are considered to be representative of the entire analysis period. For the majority of the analysis period (80% of the time), daily mean loadings were between $5\text{--}15\ \mu\text{g}\ \text{sm}^{-3}$. High pollution episodes are accordingly defined as those when the daily mean exceeds $15\ \mu\text{g}\ \text{sm}^{-3}$. Such episodes occur on 106 days out of the 534 days during the considered analysis period. Flight days where this value was exceeded are extracted for further analysis and are summarized in Table 2. Five flights in total are extracted. The average synoptic situation, derived from ECMWF geopotential height fields (not shown), for these flights consists of high pressure situated across much of the UK region. This is consistent with a relatively stagnant or recirculating air mass

Vertical distribution of sub-micron aerosol chemical composition

W. T. Morgan et al.

Title Page

Abstract

Introduction

Conclusions

References

Tables

Figures

⏪

⏩

◀

▶

Back

Close

Full Screen / Esc

Printer-friendly Version

Interactive Discussion

advecting European pollution outflow to the UK.

Figure 9 displays the median and 75th percentile mass concentrations of chemical composition as a function of height for the high pollution episode data. Nitrate mass fraction for the pollution episode data and the full dataset are also shown. The data is consistent with the ground-based data from Harwell with increased mass concentrations detected from the aircraft during the high pollution cases compared to the full dataset. This is consistent with the air mass history analysis in Sect. 3.2 with enhanced mass concentrations due to the large availability of sources in continental Europe. For the full dataset, sulphate and organics are the dominant components, with concentrations of less than $1.6 \mu\text{g sm}^{-3}$ each close to the surface. Nitrate accounts for a small fraction of the sub-micron mass. For the high pollution cases, all components are enhanced relative to the full dataset. In particular, nitrate is significantly enhanced for both the median and 75th percentile mass loading. For the 75th percentile high pollution cases, nitrate is the dominant chemical constituent between 0–1000 m, with nitrate mass concentrations exceeding $5 \mu\text{g sm}^{-3}$. Thus, the nitrate mass concentration is enhanced by a factor of 10 for the high pollution cases relative to the full dataset. Below 3000 m, nitrate is the dominant inorganic constituent. These characteristics are consistent with Sect. 3.1, with the high mass concentrations being quite distinct from the general background trend. Such high pollution episodes are coincident with considerable enhancements in the nitrate mass concentration and occurred on average 20% of the time during the flying period (5 April 2005 to 27 September 2006) considered by this analysis.

4 Conclusions

The vertical distribution of aerosol chemical composition has been characterised for the UK region. A back trajectory cluster analysis formed the basis for categorizing the source history of the aerosol properties. A key general feature of the profiles is the trend showing a relatively consistent background primarily composed of organic

Vertical distribution of sub-micron aerosol chemical composition

W. T. Morgan et al.

Title Page

Abstract

Introduction

Conclusions

References

Tables

Figures

⏪

⏩

◀

▶

Back

Close

Full Screen / Esc

Printer-friendly Version

Interactive Discussion

matter and ammonium sulphate. The background mass concentrations are similar to those measured by Coe et al. (2006) on the west coast of Ireland during westerly conditions. Enhanced organic matter concentrations are infrequently observed in the mid-troposphere, likely a result of long-range transport. The background profiles for the Atlantic cluster are representative of the input of aerosol to Western Europe. The Atlantic cluster represented the predominant condition (53% of all back trajectories) of the cluster solution. Such profiles should serve as a useful constraint for modelling studies. Summary statistics for the vertical profiles are presented in the supplementary material section (see <http://www.atmos-chem-phys-discuss.net/9/9117/2009/acpd-9-9117-2009-supplement.pdf>) for the full dataset and the cluster solutions. The background trend is punctuated by higher concentrations associated with pollution plumes. Such plumes are shown to be more intense and more frequent during periods of European outflow and periods of stagnant/recirculating air masses. Analysis of the UK surface-based measurement network corroborates this conclusion, with pollution episodes occurring on average 20% of the time during the flying period. Furthermore, Abdalmogith and Harrison (2005) showed enhanced mass concentrations during periods of European outflow compared to inflow from the Atlantic. Consequently, differing meteorological regimes have a substantial impact upon the concentration, composition and microphysical properties of the aerosol input to the UK region. Such conditions increase the prospect of maximum mass concentration targets being exceeded and amplified perturbations of the radiative equilibrium in the UK region. This has major implications for source apportionment and impact studies.

A major facet of the enhanced mass concentrations observed was the increase in the fractional contribution of nitrate to the particulate mass. This is consistent with previous composition profiles derived from AMS measurements in Europe (Crosier et al., 2007; Schneider et al., 2006). This was particularly evident when assigning high pollution episodes based upon the surface-based data and the general features of the European outflow cluster. Furthermore, nitrate was shown to exhibit more variability as a function of height within the boundary layer compared to organic matter and sulphate.

**Vertical distribution
of sub-micron
aerosol chemical
composition**W. T. Morgan et al.

Title Page

Abstract

Introduction

Conclusions

References

Tables

Figures

⏪

⏩

◀

▶

Back

Close

Full Screen / Esc

Printer-friendly Version

Interactive Discussion

Nitrate exhibited two maxima within the boundary layer; one close to the surface and a second close to the top of the boundary layer. Formation occurring higher in the boundary layer is likely due to thermodynamics driving the chemical partitioning of the gas phase precursors to the particle phase. Such effects have previously been observed on the west coast of the USA (Neuman et al., 2003) and demonstrated using 1-D thermodynamic modelling above Tokyo, Japan (Morino et al., 2006). On the regional scale, organic matter is predominantly composed of Secondary Organic Aerosol (SOA) under polluted conditions in the Northern Hemisphere (Zhang et al., 2007), which potentially contains a significant semi-volatile fraction (Donahue et al., 2006). Whether the organic matter displays similar semi-volatile behaviour to the nitrate is unclear from this dataset. The dataset does indicate that ammonium nitrate can be a substantial component of the regional aerosol burden. Its complex vertical distribution highlights the requirement for accurate representation of aerosol formation and processes away from the surface.

These findings have significant implications for treatment of the radiative and ecological effects of anthropogenic aerosol. Firstly, the addition of relatively more inorganic material to a mixed inorganic-organic system will enhance the hygroscopic nature of the aerosol. Consequently, the addition of particulate mass coupled with enhanced hygroscopicity will greatly enhance the Aerosol Optical Depth (AOD) of the atmospheric burden. Such impacts will be exacerbated in areas exhibiting high relative humidity, such as the top of the boundary layer. The deliquescence relative humidity of ammonium nitrate is 62% (Tang, 1996) with a growth factor of 1.59 at a relative humidity of 85% (Topping et al., 2005), thus the wet size of the aerosol is enhanced. Such effects combine to greatly increase the scattering potential of the aerosol, increasing the magnitude of the aerosol direct effect. Secondly, clouds forming at the top of the boundary layer entrain air from beneath them into the cloud. Enhanced ammonium nitrate concentrations in such air will lead to a modification of the microphysical properties of the cloud. Such modifications are known to modify the amount, lifetime and radiative impact of clouds, the so-called indirect effect of aerosols (e.g. McFiggans et al., 2006).

**Vertical distribution
of sub-micron
aerosol chemical
composition**

W. T. Morgan et al.

Title Page

Abstract

Introduction

Conclusions

References

Tables

Figures

⏪

⏩

◀

▶

Back

Close

Full Screen / Esc

Printer-friendly Version

Interactive Discussion

**Vertical distribution
of sub-micron
aerosol chemical
composition**W. T. Morgan et al.

[Title Page](#)[Abstract](#)[Introduction](#)[Conclusions](#)[References](#)[Tables](#)[Figures](#)[⏪](#)[⏩](#)[◀](#)[▶](#)[Back](#)[Close](#)[Full Screen / Esc](#)[Printer-friendly Version](#)[Interactive Discussion](#)

As well as such climate related impacts, nitrate partitioning significantly perturbs the nitrogen cycle of the atmosphere. Particulate nitrate has a dry deposition velocity which is ten times slower than that of nitric acid (Seinfeld and Pandis, 1998). Consequently, transport and ultimately deposition can be substantially altered by this partitioning phenomenon. Further elucidation of the impact of ammonium nitrate is required across Europe, particularly in terms of its direct and indirect radiative effects.

Acknowledgements. We would like to acknowledge the efforts of FAAM, DirectFlight, Avalon and the Met Office and everyone associated with the various projects from which data was used for this study. W. T. Morgan was supported by a Natural Environment Research Council (NERC) studentship NER/S/A/2006/14040 and a CASE sponsorship from Aerodyne Research Inc. The NERC National Centre for Atmospheric Science (NCAS) Facility for Ground based Atmospheric Measurements (FGAM) supported the maintenance of the Q-AMS. NCAS also supported the development of the data interpretation methods employed here through its Composition Directorate. Several NERC funded projects were used in this study including AMPEP (NER/T/S/2002/00493), CIRRUS (NER/T/S/2002/00135), CLOPAP (NER/T/S/2002/00147) and ICEPIC (NER/A/S/2002/01021). Thanks to the British Atmospheric Data Centre (BADC) for the calculation of trajectories and access to ECMWF data. The UK Air Quality Archive website is prepared and hosted by AEA Energy & Environment, on behalf of the UK Department for Environment, Food & Rural Affairs and the Devolved Administrations. We also thank G. McFiggans and G. R. McMeeking for useful critical comments.

References

- Abdalmogith, S. S. and Harrison, R. M.: The use of trajectory cluster analysis to examine the long-range transport of secondary inorganic aerosol in the UK, *Atmos. Environ.*, 39, 6686–6695, 2005. 9120, 9132
- Allan, J. D., Jimenez, J. L., Williams, P. I., Alfarra, M. R., Bower, K. N., Jayne, J. T., Coe, H., and Worsnop, D. R.: Quantitative sampling using an Aerodyne aerosol mass spectrometer – 1. Techniques of data interpretation and error analysis, *J. Geophys. Res.-Atmos.*, 108, 4090, doi:10.1029/2002JD002358, 2003. 9121

**Vertical distribution
of sub-micron
aerosol chemical
composition**W. T. Morgan et al.

- Allan, J. D., Delia, A. E., Coe, H., Bower, K. N., Alfarra, M. R., Jimenez, J. L., Middlebrook, A. M., Drewnick, F., Onasch, T. B., Canagaratna, M. R., Jayne, J. T., and Worsnop, D. R.: A generalised method for the extraction of chemically resolved mass spectra from aerodyne aerosol mass spectrometer data, *J. Aerosol Sci.*, 35, 909–922, 2004. 9121
- 5 Bahreini, R., Jimenez, J. L., Wang, J., Flagan, R. C., Seinfeld, J. H., Jayne, J. T., and Worsnop, D. R.: Aircraft-based aerosol size and composition measurements during ACE-Asia using an Aerodyne aerosol mass spectrometer, *J. Geophys. Res.-Atmos.*, 108, 8645, doi:10.1029/2002JD003226, 2003. 9119
- Canagaratna, M. R., Jayne, J. T., Jimenez, J. L., Allan, J. D., Alfarra, M. R., Zhang, Q., Onasch, T. B., Drewnick, F., Coe, H., Middlebrook, A., Delia, A., Williams, L. R., Trimborn, A. M., Northway, M. J., DeCarlo, P. F., Kolb, C. E., Davidovits, P., and Worsnop, D. R.: Chemical and microphysical characterization of ambient aerosols with the aerodyne aerosol mass spectrometer, *Mass Spectrom. Rev.*, 26, 185–222, 2007. 9119
- 10 Cape, J. N., Methven, J., and Hudson, L. E.: The use of trajectory cluster analysis to interpret trace gas measurements at Mace Head, Ireland, *Atmos. Environ.*, 34, 3651–3663, 2000. 9124
- Coe, H., Allan, J. D., Alfarra, M. R., Bower, K. N., Flynn, M. J., McFiggans, G. B., Topping, D. O., Williams, P. I., O'Dowd, C. D., Dall'Osto, M., Beddows, D. C. S., and Harrison, R. M.: Chemical and physical characteristics of aerosol particles at a remote coastal location, Mace Head, Ireland, during NAMBLEX, *Atmos. Chem. Phys.*, 6, 3289–3301, 2006, <http://www.atmos-chem-phys.net/6/3289/2006/>. 9120, 9132
- 20 Crosier, J., Allan, J. D., Coe, H., Bower, K. N., Formenti, P., and Williams, P. I.: Chemical composition of summertime aerosol in the Po Valley (Italy), northern Adriatic and Black Sea, *Q. J. Roy. Meteorol. Soc.*, 133, 61–75, suppl. 1, 2007. 9119, 9121, 9132
- 25 DeCarlo, P. F., Slowik, J. G., Worsnop, D. R., Davidovits, P., and Jimenez, J. L.: Particle morphology and density characterization by combined mobility and aerodynamic diameter measurements. Part 1: Theory, *Aerosol Sci. Technol.*, 38, 1185–1205, 2004. 9122
- Donahue, N. M., Robinson, A. L., Stanier, C. O., and Pandis, S. N.: Coupled partitioning, dilution, and chemical aging of semivolatile organics, *Environ. Sci. Technol.*, 40, 2635–2643, 2006. 9133
- 30 Foltescu, V. L., Selin, E., and Below, M.: Corrections for Particle Losses and Sizing Errors During Aircraft Aerosol Sampling Using a Rosemount Inlet and the Pms Las-X, *Atmos. Environ.*, 29, 449–453, 1995. 9122

[Title Page](#)[Abstract](#)[Introduction](#)[Conclusions](#)[References](#)[Tables](#)[Figures](#)[⏪](#)[⏩](#)[◀](#)[▶](#)[Back](#)[Close](#)[Full Screen / Esc](#)[Printer-friendly Version](#)[Interactive Discussion](#)

**Vertical distribution
of sub-micron
aerosol chemical
composition**

W. T. Morgan et al.

Title Page

Abstract

Introduction

Conclusions

References

Tables

Figures

◀

▶

◀

▶

Back

Close

Full Screen / Esc

Printer-friendly Version

Interactive Discussion

- Forster, P., Ramaswamy, V., Artaxo, P., Berntsen, T., Betts, R., Fahey, D.W., Haywood, J., Lean, J., Lowe, D., Myhre, G., Nganga, J., Prinn, R., Raga, G., Schulz, M., and Van Dorland, R.: Changes in Atmospheric Constituents and in Radiative Forcing, *Climate Change 2007: The Physical Science Basis. Contribution of Working Group I to the Fourth Assessment Report of the Intergovernmental Panel on Climate Change*, Cambridge University Press, Cambridge, United Kingdom and New York, NY, USA, 2007. 9118, 9119
- Haywood, J. and Boucher, O.: Estimates of the direct and indirect radiative forcing due to tropospheric aerosols: A review, *Rev. Geophys.*, 38, 513–543, 2000. 9119
- Jayne, J. T., Leard, D. C., Zhang, X. F., Davidovits, P., Smith, K. A., Kolb, C. E., and Worsnop, D. R.: Development of an aerosol mass spectrometer for size and composition analysis of submicron particles, *Aerosol Sci. Technol.*, 33, 49–70, 2000. 9119, 9121
- Jimenez, J. L., Jayne, J. T., Shi, Q., Kolb, C. E., Worsnop, D. R., Yourshaw, I., Seinfeld, J. H., Flagan, R. C., Zhang, X. F., Smith, K. A., Morris, J. W., and Davidovits, P.: Ambient aerosol sampling using the Aerodyne Aerosol Mass Spectrometer, *J. Geophys. Res.-Atmos.*, 108, 8425, doi:10.1029/2001JD001213, 2003. 9121
- Kalkstein, L. S., Tan, G. R., and Skindlov, J. A.: An Evaluation of 3 Clustering Procedures for Use in Synoptic Climatological Classification, *J. Clim. Appl. Meteorol.*, 26, 717–730, 1987. 9124
- Kinne, S., Schulz, M., Textor, C., Guibert, S., Balkanski, Y., Bauer, S. E., Berntsen, T., Berglen, T. F., Boucher, O., Chin, M., Collins, W., Dentener, F., Diehl, T., Easter, R., Feichter, J., Fillmore, D., Ghan, S., Ginoux, P., Gong, S., Grini, A., Hendricks, J., Herzog, M., Horowitz, L., Isaksen, I., Iversen, T., Kirkevåg, A., Kloster, S., Koch, D., Kristjansson, J. E., Krol, M., Lauer, A., Lamarque, J. F., Lesins, G., Liu, X., Lohmann, U., Montanaro, V., Myhre, G., Penner, J., Pitari, G., Reddy, S., Seland, O., Stier, P., Takemura, T., and Tie, X.: An AeroCom initial assessment optical properties in aerosol component modules of global models, *Atmos. Chem. Phys.*, 6, 1815–1834, 2006, <http://www.atmos-chem-phys.net/6/1815/2006/>. 9119
- Lee, Y. N., Weber, R., Ma, Y., Orsini, D., Maxwell-Meier, K., Blake, D., Meinardi, S., Sachse, G., Harward, C., Chen, T. Y., Thornton, D., Tu, F. H., and Bandy, A.: Airborne measurement of inorganic ionic components of fine aerosol particles using the particle-into-liquid sampler coupled to ion chromatography technique during ACE-Asia and TRACE-P, *J. Geophys. Res.-Atmos.*, 108, 8646, doi:10.1029/2002JD003265, 2003. 9119
- Liu, P., Ziemann, P. J., Kittelson, D. B., and McMurry, P. H.: Generating Particle Beams of

**Vertical distribution
of sub-micron
aerosol chemical
composition**

W. T. Morgan et al.

Title Page

Abstract

Introduction

Conclusions

References

Tables

Figures

⏪

⏩

◀

▶

Back

Close

Full Screen / Esc

Printer-friendly Version

Interactive Discussion

Controlled Dimensions and Divergence. 1. Theory of Particle Motion in Aerodynamic Lenses and Nozzle Expansions, *Aerosol Sci. Technol.*, 22, 293–313, 1995a. 9122

Liu, P., Ziemann, P. J., Kittelson, D. B., and McMurry, P. H.: Generating Particle Beams of Controlled Dimensions and Divergence .2. Experimental Evaluation of Particle Motion in Aerodynamic Lenses and Nozzle Expansions, *Aerosol Sci. Technol.*, 22, 314–324, 1995b. 9122

Liu, P. S. K., Leaitch, W. R., Strapp, J. W., and Wasey, M. A.: Response of Particle Measuring Systems Airborne ASAP and PCASP to NaCl and Latex-Particles, *Aerosol Sci. Technol.*, 16, 83–95, 1992. 9121

Matthew, B. M., Middlebrook, A. M., and Onasch, T. B.: Collection efficiencies in an Aerodyne Aerosol Mass Spectrometer as a function of particle phase for laboratory generated aerosols, *Aerosol Sci. Technol.*, 42, 884–898, iSI Document Delivery No.: 353ULTimes Cited: 1Cited Reference Count: 59, 2008. 9121

McFiggans, G., Artaxo, P., Baltensperger, U., Coe, H., Facchini, M. C., Feingold, G., Fuzzi, S., Gysel, M., Laaksonen, A., Lohmann, U., Mentel, T. F., Murphy, D. M., O'Dowd, C. D., Snider, J. R., and Weingartner, E.: The effect of physical and chemical aerosol properties on warm cloud droplet activation, *Atmos. Chem. Phys.*, 6, 2593–2649, 2006, <http://www.atmos-chem-phys.net/6/2593/2006/>. 9133

Morino, Y., Kondo, Y., Takegawa, N., Miyazaki, Y., Kita, K., Komazaki, Y., Fukuda, M., Miyakawa, T., Moteki, N., and Worsnop, D. R.: Partitioning of HNO₃ and particulate nitrate over Tokyo: Effect of vertical mixing, *J. Geophys. Res.-Atmos.*, 111, D15215, doi:10.1029/2005JD006887, 2006. 9119, 9133

Mozurkewich, M.: The Dissociation-Constant of Ammonium-Nitrate and Its Dependence on Temperature, Relative-Humidity and Particle-Size, *Atmos. Environ. Part A-Gen.*, 27, 261–270, 1993. 9120

Neuman, J. A., Nowak, J. B., Brock, C. A., Trainer, M., Fehsenfeld, F. C., Holloway, J. S., Hubler, G., Hudson, P. K., Murphy, D. M., Nicks, D. K., Orsini, D., Parrish, D. D., Ryerson, T. B., Sueper, D. T., Sullivan, A., and Weber, R.: Variability in ammonium nitrate formation and nitric acid depletion with altitude and location over California, *J. Geophys. Res.-Atmos.*, 108, 4557, doi:10.1029/2003JD003616, 2003. 9119, 9133

Orsini, D. A., Ma, Y. L., Sullivan, A., Sierau, B., Baumann, K., and Weber, R. J.: Refinements to the particle-into-liquid sampler (PILS) for ground and airborne measurements of water soluble aerosol composition, *Atmos. Environ.*, 37, 1243–1259, 2003. 9119

Osborne, S. R. and Haywood, J. M.: Aircraft observations of the microphysical and optical properties of major aerosol species, *Atmos. Res.*, 73, 173–201, iSI Document Delivery No.: 898CNTimes Cited: 5Cited Reference Count: 46, 2005. 9129

Schneider, J., Hings, S. S., Hock, B. N., Weimer, S., Borrmann, S., Fiebig, M., Petzold, A., Busen, R., and Karcher, B.: Aircraft-based operation of an aerosol mass spectrometer: Measurements of tropospheric aerosol composition, *J. Aerosol Sci.*, 37, 839–857, 2006. 9119, 9132

Schulz, M., Textor, C., Kinne, S., Balkanski, Y., Bauer, S., Berntsen, T., Berglen, T., Boucher, O., Dentener, F., Guibert, S., Isaksen, I. S. A., Iversen, T., Koch, D., Kirkevåg, A., Liu, X., Montanaro, V., Myhre, G., Penner, J. E., Pitari, G., Reddy, S., Seland, Ø., Stier, P., and Takemura, T.: Radiative forcing by aerosols as derived from the AeroCom present-day and pre-industrial simulations, *Atmos. Chem. Phys.*, 6, 5225–5246, 2006, <http://www.atmos-chem-phys.net/6/5225/2006/>. 9119

Seinfeld, J. H. and Pandis, S.: *Atmospheric chemistry and physics: from air pollution to climate change*, John Wiley & Sons, New York, USA, 1998. 9134

Stelson, A. W. and Seinfeld, J. H.: Relative-Humidity and Ph-Dependence of the Vapor-Pressure of Ammonium-Nitrate Nitric Acid-Solutions at 25-Degrees-C, *Atmos. Environ.*, 16, 993–1000, 1982. 9120

Strapp, J. W., Leaitch, W. R., and Liu, P. S. K.: Hydrated and Dried Aerosol-Size-Distribution Measurements from the Particle Measuring Systems FSSP-300 Probe and the Deiced PCASP-100x Probe, *J. Atmos. Ocean. Tech.*, 9, 548–555, 1992. 9121

Tang, I. N.: Chemical and size effects of hygroscopic aerosols on light scattering coefficients, *J. Geophys. Res.-Atmos.*, 101, 19245–19250, 1996. 9133

Textor, C., Schulz, M., Guibert, S., Kinne, S., Balkanski, Y., Bauer, S., Berntsen, T., Berglen, T., Boucher, O., Chin, M., Dentener, F., Diehl, T., Easter, R., Feichter, H., Fillmore, D., Ghan, S., Ginoux, P., Gong, S., Grini, A., Hendricks, J., Horowitz, L., Huang, P., Isaksen, I., Iversen, I., Kloster, S., Koch, D., Kirkevåg, A., Kristjansson, J. E., Krol, M., Lauer, A., Lamarque, J. F., Liu, X., Montanaro, V., Myhre, G., Penner, J., Pitari, G., Reddy, S., Seland, Ø., Stier, P., Takemura, T., and Tie, X.: Analysis and quantification of the diversities of aerosol life cycles within AeroCom, *Atmos. Chem. Phys.*, 6, 1777–1813, 2006, <http://www.atmos-chem-phys.net/6/1777/2006/>. 9119

Topping, D. O., McFiggans, G. B., and Coe, H.: A curved multi-component aerosol hygroscopicity model framework: Part 1 – Inorganic compounds, *Atmos. Chem. Phys.*, 5, 1205–1222,

**Vertical distribution
of sub-micron
aerosol chemical
composition**W. T. Morgan et al.

[Title Page](#)[Abstract](#)[Introduction](#)[Conclusions](#)[References](#)[Tables](#)[Figures](#)[⏪](#)[⏩](#)[◀](#)[▶](#)[Back](#)[Close](#)[Full Screen / Esc](#)[Printer-friendly Version](#)[Interactive Discussion](#)

2005,

<http://www.atmos-chem-phys.net/5/1205/2005/>. 9133

Weber, R. J., Orsini, D., Daun, Y., Lee, Y. N., Klotz, P. J., and Brechtel, F.: A particle-into-liquid collector for rapid measurement of aerosol bulk chemical composition, *Aerosol Sci. Technol.*, 35, 718–727, 2001. 9119

Zhang, Q., Jimenez, J. L., Canagaratna, M. R., Allan, J. D., Coe, H., Ulbrich, I., Alfarra, M. R., Takami, A., Middlebrook, A. M., Sun, Y. L., Dzepina, K., Dunlea, E., Docherty, K., DeCarlo, P. F., Salcedo, D., Onasch, T., Jayne, J. T., Miyoshi, T., Shimonono, A., Hatakeyama, S., Takegawa, N., Kondo, Y., Schneider, J., Drewnick, F., Borrmann, S., Weimer, S., Demerjian, K., Williams, P., Bower, K., Bahreini, R., Cottrell, L., Griffin, R. J., Rautiainen, J., Sun, J. Y., Zhang, Y. M., and Worsnop, D. R.: Ubiquity and dominance of oxygenated species in organic aerosols in anthropogenically-influenced Northern Hemisphere midlatitudes, *Geophys. Res. Lett.*, 34, L13801, doi:10.1029/2007GL029979, 2007. 9133

Zhang, X. F., Smith, K. A., Worsnop, D. R., Jimenez, J., Jayne, J. T., and Kolb, C. E.: A numerical characterization of particle beam collimation by an aerodynamic lens-nozzle system: Part I. An individual lens or nozzle, *Aerosol Sci. Technol.*, 36, 617–631, 2002. 9122

ACPD

9, 9117–9150, 2009

**Vertical distribution
of sub-micron
aerosol chemical
composition**

W. T. Morgan et al.

Title Page

Abstract

Introduction

Conclusions

References

Tables

Figures

◀

▶

◀

▶

Back

Close

Full Screen / Esc

Printer-friendly Version

Interactive Discussion

**Vertical distribution
of sub-micron
aerosol chemical
composition**

W. T. Morgan et al.

Table 1. Summary of cluster solution including details of the number of profiles, SLRs and back trajectories associated with each cluster.

Cluster	Condition	Profiles	SLRs	Back Trajectories
1	Atlantic origin	181	51	84
2	Easterly	44	19	19
3	Southerly	18	7	6
4	Northerly	29	N/A	18
5	Stagnant air masses	67	5	32

[Title Page](#)[Abstract](#)[Introduction](#)[Conclusions](#)[References](#)[Tables](#)[Figures](#)[I◀](#)[▶I](#)[◀](#)[▶](#)[Back](#)[Close](#)[Full Screen / Esc](#)[Printer-friendly Version](#)[Interactive Discussion](#)

**Vertical distribution
of sub-micron
aerosol chemical
composition**

W. T. Morgan et al.

Table 2. Details of flights which occurred when daily mean $\text{PM}_{2.5}$ measurements at Harwell, UK exceeded $15 \mu\text{g sm}^{-3}$.

Date	Flight Number	$\text{PM}_{2.5}$ Mass Concentration ($\mu\text{g sm}^{-3}$)
21/04/2005	B091	16
13/07/2005	B110	16
17/08/2005	B122	17
22/09/2005	B133	16
12/05/2006	B198	21

Title Page

Abstract

Introduction

Conclusions

References

Tables

Figures

I◀

▶I

◀

▶

Back

Close

Full Screen / Esc

Printer-friendly Version

Interactive Discussion

**Vertical distribution
of sub-micron
aerosol chemical
composition**

W. T. Morgan et al.

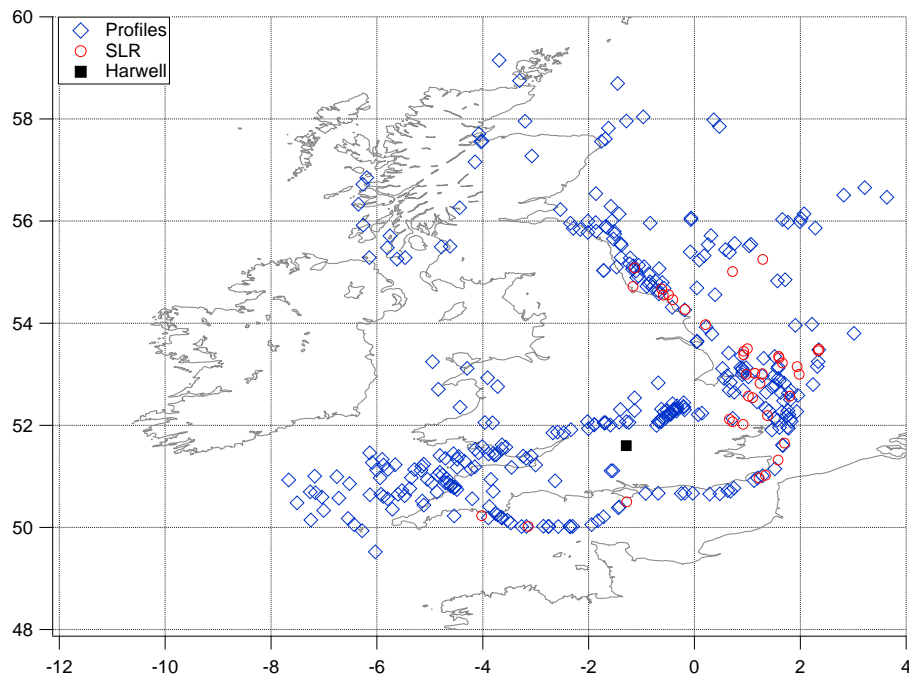


Fig. 1. Location of vertical profiles and constant altitude straight and level runs (SLRs). The latitude/longitude grid marks out the sectors referred to in Sect. 2.2. The location of the ground-based monitoring station at Harwell is also shown.

[Title Page](#)[Abstract](#)[Introduction](#)[Conclusions](#)[References](#)[Tables](#)[Figures](#)[◀](#)[▶](#)[◀](#)[▶](#)[Back](#)[Close](#)[Full Screen / Esc](#)[Printer-friendly Version](#)[Interactive Discussion](#)

**Vertical distribution
of sub-micron
aerosol chemical
composition**

W. T. Morgan et al.

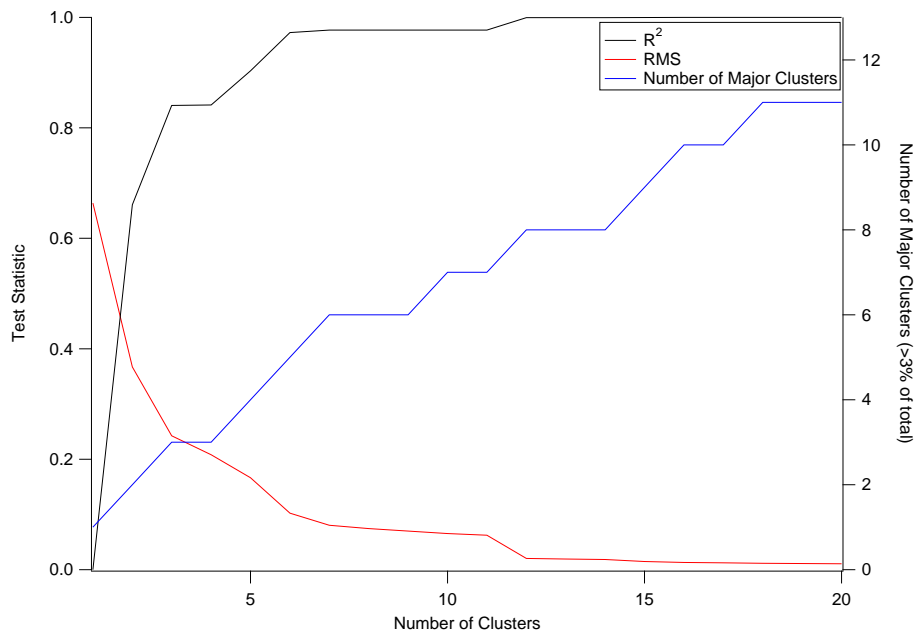


Fig. 2. Variation in R^2 and RMS as a function of the number of clusters. The number of major clusters is also shown which is defined as clusters containing more than 3% of the total back trajectories.

[Title Page](#)[Abstract](#)[Introduction](#)[Conclusions](#)[References](#)[Tables](#)[Figures](#)[⏪](#)[⏩](#)[◀](#)[▶](#)[Back](#)[Close](#)[Full Screen / Esc](#)[Printer-friendly Version](#)[Interactive Discussion](#)

**Vertical distribution
of sub-micron
aerosol chemical
composition**

W. T. Morgan et al.

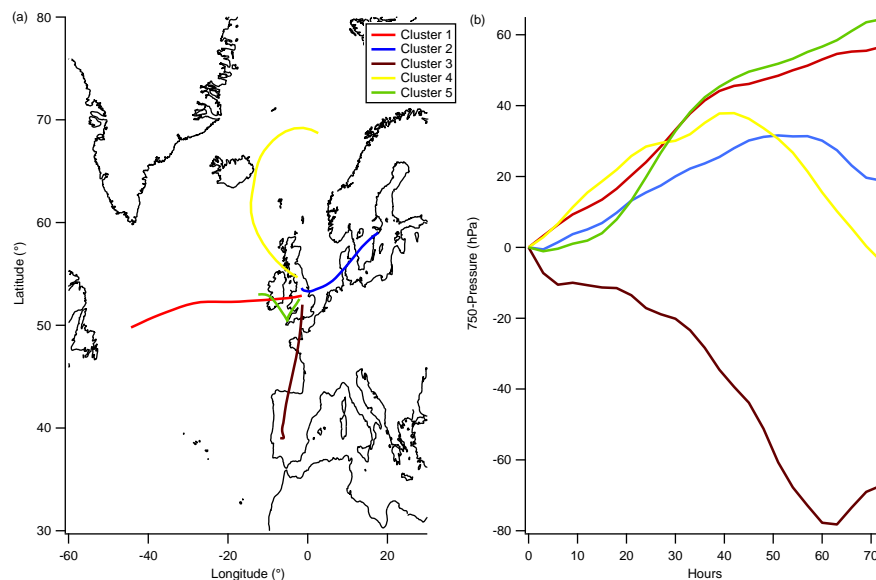


Fig. 3. (a) Mean back trajectories for the five cluster solution at six-hourly time steps. (b) Mean back trajectories for the five cluster solution displaying the vertical deviation for an air mass with six-hourly time steps. Positive values indicate that an air mass has descended at a time step.

[Title Page](#)[Abstract](#)[Introduction](#)[Conclusions](#)[References](#)[Tables](#)[Figures](#)[◀](#)[▶](#)[◀](#)[▶](#)[Back](#)[Close](#)[Full Screen / Esc](#)[Printer-friendly Version](#)[Interactive Discussion](#)

**Vertical distribution
of sub-micron
aerosol chemical
composition**

W. T. Morgan et al.

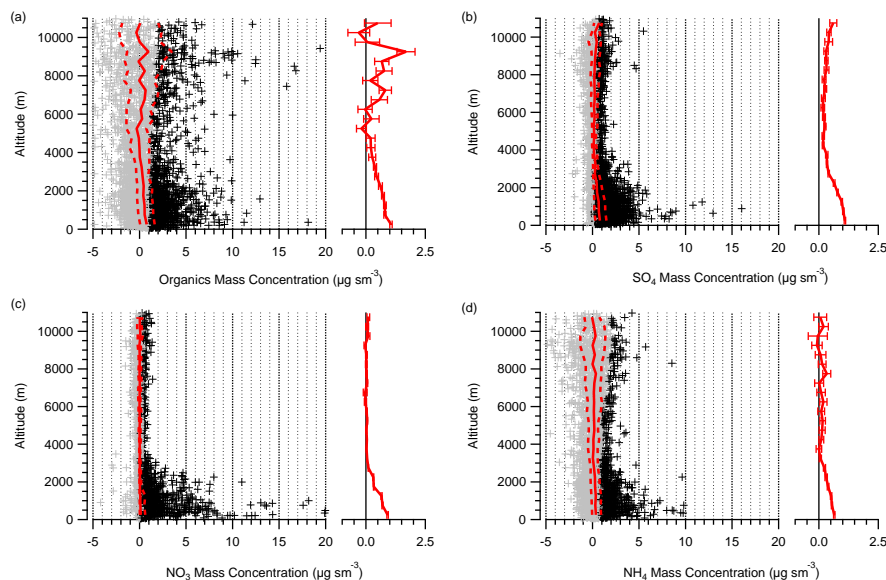


Fig. 4. Vertical profiles of aerosol chemical composition from the AMS for the UK for each chemical species. Black crosses are individual data points above the 2σ profile for each species whilst grey crosses correspond to those below. Red lines are the 25th, 50th and 75th percentiles for 500 m altitude bins. On the right hand side panel for each species the red line shows the mean for each altitude bin with the horizontal bar indicating the variability about the mean value, defined in Sect. 3.1. Tabulated statistics are available in the supporting material (see: <http://www.atmos-chem-phys-discuss.net/9/9117/2009/acpd-9-9117-2009-supplement.pdf>).

Title Page

Abstract

Introduction

Conclusions

References

Tables

Figures

◀

▶

◀

▶

Back

Close

Full Screen / Esc

Printer-friendly Version

Interactive Discussion

**Vertical distribution
of sub-micron
aerosol chemical
composition**

W. T. Morgan et al.

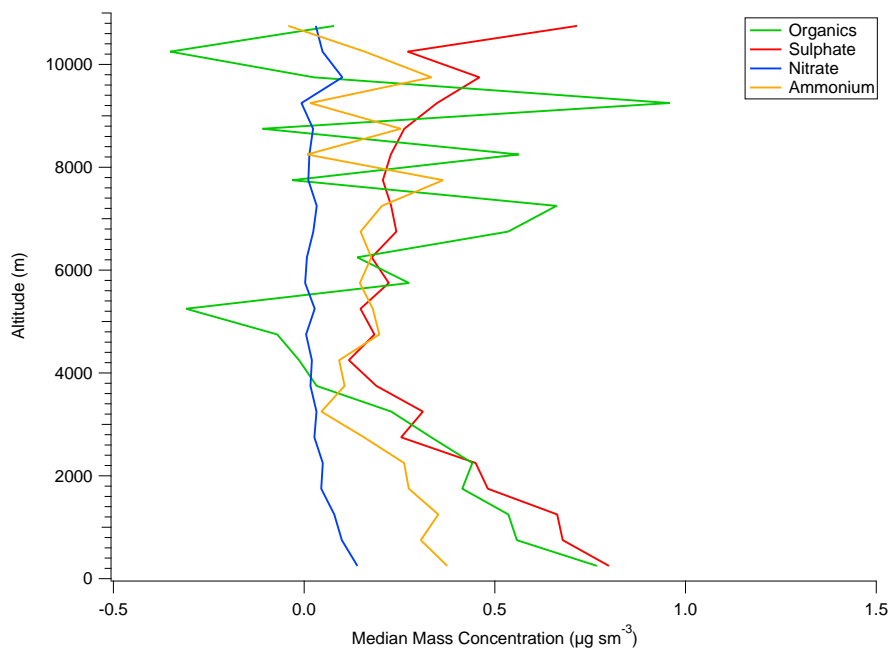


Fig. 5. Sulphate, organics, nitrate and ammonium median mass concentration profiles for the full dataset.

[Title Page](#)[Abstract](#)[Introduction](#)[Conclusions](#)[References](#)[Tables](#)[Figures](#)[◀](#)[▶](#)[◀](#)[▶](#)[Back](#)[Close](#)[Full Screen / Esc](#)[Printer-friendly Version](#)[Interactive Discussion](#)

**Vertical distribution
of sub-micron
aerosol chemical
composition**

W. T. Morgan et al.

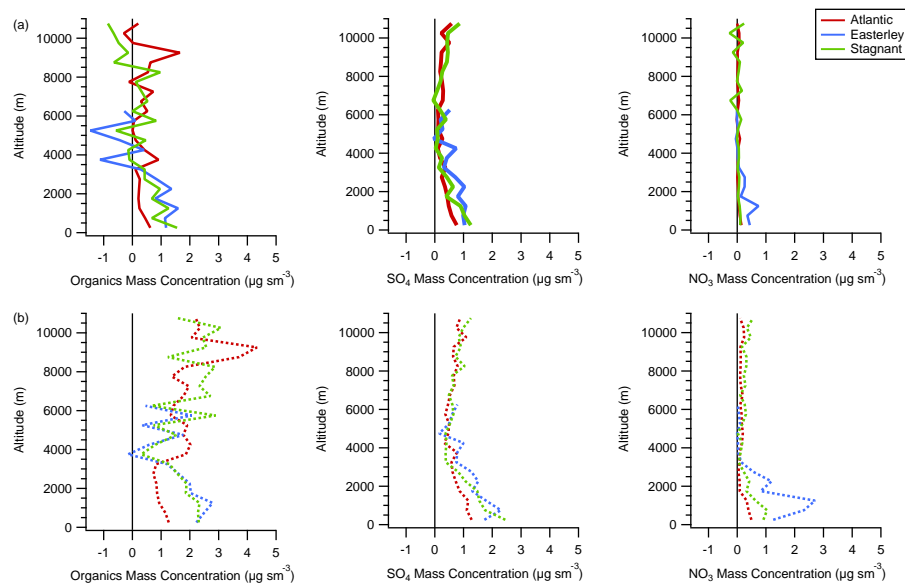


Fig. 6. (a) shows the median mass concentration profiles for the clusters for organics, sulphate and nitrate and (b) displays the corresponding 75th percentile mass concentration profiles. The legend indicates the respective cluster. Tabulated statistics are available in the supporting material (see <http://www.atmos-chem-phys-discuss.net/9/9117/2009/acpd-9-9117-2009-supplement.pdf>).

Title Page

Abstract

Introduction

Conclusions

References

Tables

Figures

◀

▶

◀

▶

Back

Close

Full Screen / Esc

Printer-friendly Version

Interactive Discussion

**Vertical distribution
of sub-micron
aerosol chemical
composition**

W. T. Morgan et al.

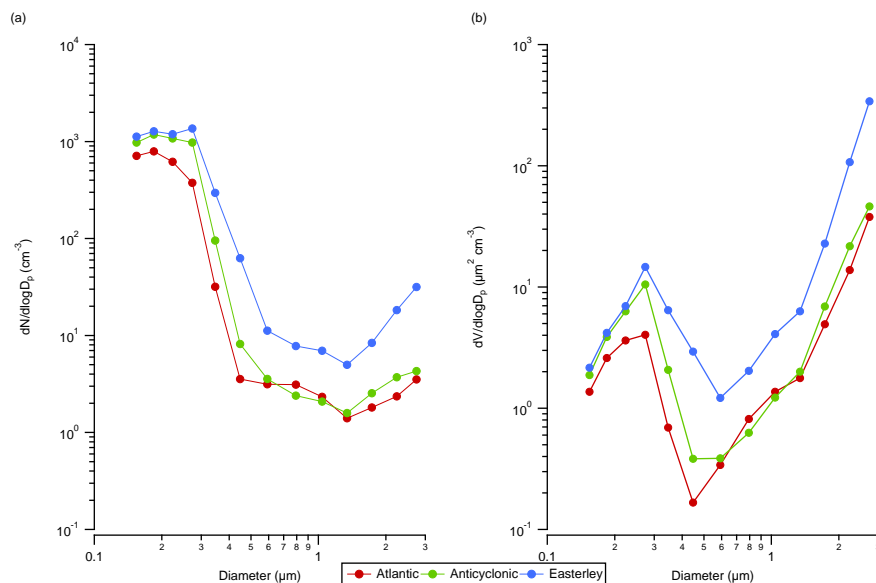


Fig. 7. Average PCASP size distributions for **(a)** number and **(b)** volume. The legend indicates the respective clusters the distributions are averaged over.

[Title Page](#)[Abstract](#)[Introduction](#)[Conclusions](#)[References](#)[Tables](#)[Figures](#)[◀](#)[▶](#)[◀](#)[▶](#)[Back](#)[Close](#)[Full Screen / Esc](#)[Printer-friendly Version](#)[Interactive Discussion](#)

**Vertical distribution
of sub-micron
aerosol chemical
composition**

W. T. Morgan et al.

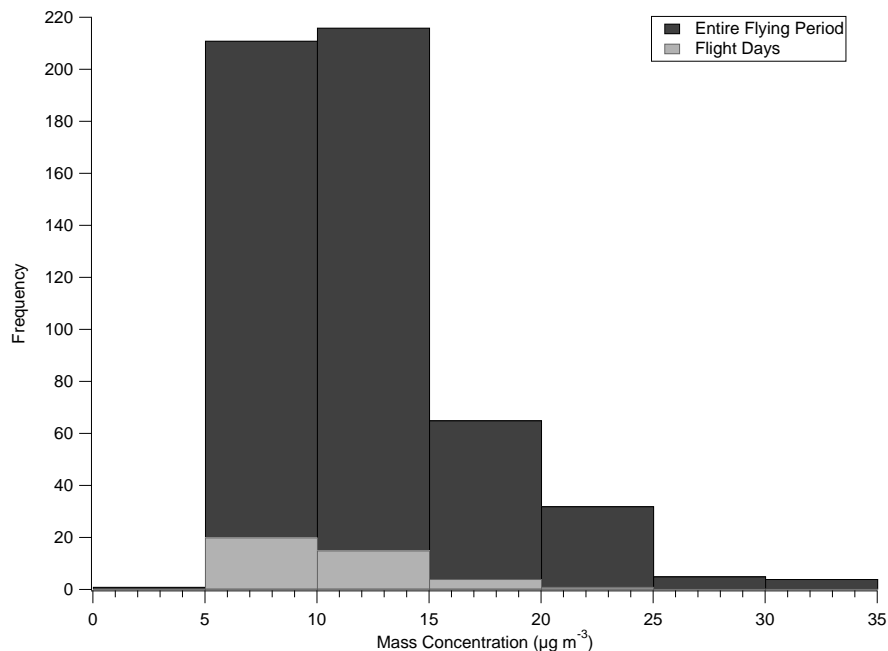


Fig. 8. Histogram of daily mean $\text{PM}_{2.5}$ mass concentrations at Harwell for the entire flying period (5 April 2005 to 27 September 2006) covered by this study and the individual flight days.

[Title Page](#)[Abstract](#)[Introduction](#)[Conclusions](#)[References](#)[Tables](#)[Figures](#)[◀](#)[▶](#)[◀](#)[▶](#)[Back](#)[Close](#)[Full Screen / Esc](#)[Printer-friendly Version](#)[Interactive Discussion](#)

Vertical distribution of sub-micron aerosol chemical composition

W. T. Morgan et al.

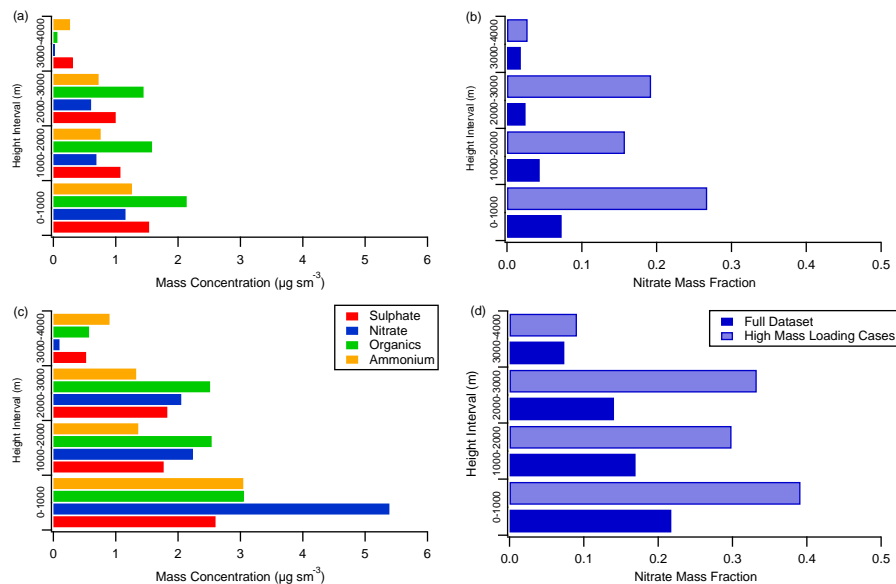


Fig. 9. Distribution of Q-AMS mass as a function of height for high mass loading cases where **(a)** represents the median mass concentration for each height interval and **(c)** represents the 75th percentile mass concentration for each height interval. **(b)** and **(d)** contrast the nitrate mass fraction for the high mass loading cases and the full dataset for the median and 75th percentile, respectively.

[Title Page](#)
[Abstract](#)
[Introduction](#)
[Conclusions](#)
[References](#)
[Tables](#)
[Figures](#)
[Back](#)
[Close](#)
[Full Screen / Esc](#)
[Printer-friendly Version](#)
[Interactive Discussion](#)